Additions and corrections

Catalytic disproportionation of *N*-alkylhydroxylamines bound to pentacyanoferrates

María M. Gutiérrez, Graciela B. Alluisetti, Carina Gaviglio, Fabio Doctorovich, José A. Olabe and Valentín T. Amorebieta*

Dalton Trans., 2009, 1187 (DOI: 10.1039/b812173g). ***Amendment published 18th March 2010*.**

In the published version of this paper the authors Carina Gaviglio and Fabio Doctorovich were inadvertently omitted from the authorship list. The complete list of author is given below:

María M. Gutiérrez,[a] Graciela B. Alluisetti,[a] Carina Gaviglio,[b] Fabio Doctorovich,[b] José A. Olabe[c] and Valentín T. Amorebieta*[a]

[a]*Department of Chemistry, Facultad de Ciencias Exactas y Naturales, Universidad Nacional de Mar del Plata, Funes y Roca, Mar del Plata, B7602AYL, Argentina. E-mail: amorebie@mdp.edu.ar*

[b]*Departamento de Química Inorgánica, Analítica y Química Física/INQUIMAE-CONICET, Facultad de Ciencias Exactas y Naturales, Universidad de Buenos Aires, Ciudad Universitaria, Pabellón II, Piso 3, C1428EHA, Buenos Aires, Argentina*

[c]*Department of Inorganic, Analytical and Physical Chemistry and INQUIMAE, CONICET, Facultad de Ciencias Exactas y Naturales, Universidad de Buenos Aires, Pabellón 2, Ciudad Universitaria, C1428EHA, Buenos Aires, Argentina*

The Royal Society of Chemistry apologises for this error and any consequent inconvenience to authors and readers.

Catalytic disproportionation of *N*-alkylhydroxylamines bound to pentacyanoferrates†

María M. Gutiérrez,[a] Graciela B. Alluisetti,[a] José A. Olabe[b] and Valentín T. Amorebieta*[a]

Received 16th July 2008, Accepted 17th October 2008
First published as an Advance Article on the web 22nd December 2008
DOI: 10.1039/b812173g

The substituted hydroxylamines, $CH_3N(H)OH$ (*N*-methylhydroxylamine) and $(CH_3)_2NOH$ (*N*,*N*-dimethylhydroxylamine), disproportionate catalytically to the corresponding alkylamines and oxidation products, only in the presence of $[Fe(CN)_5H_2O]^{3-}$. Substitution kinetic measurements suggest an initial coordination step to Fe(II). Two parallel *N*- and *O*-coordination modes are considered with the subsequent formation of Fe(III), free aminyl ($RNCH_3$) and nitroxide ($RN(CH_3)O$) radicals (R = H, CH_3). With $CH_3N(H)OH$, bound nitrosomethane, CH_3NO, has been characterized by UV-visible and IR spectroscopies. The mechanism is discussed on the basis of common and differential features with respect to the disproportionation of hydroxylamine catalyzed by the same Fe-fragment.

Introduction

Oxidation chemistry, particularly related to the industrial conversion of NH_3 to HNO_3, has attracted the attention of chemists over the years.[1] This full 8-electron conversion needs to be accomplished in several independently characterized steps, comprising the formation of NO, NO_2 and NO_2^-, to select only the main relevant *N*-containing intermediates. Related global transformations occur in soils during the enzyme-catalyzed bacterial processes associated with nitrifications and denitrifications.[2–6]

In the above context hydroxylamine (HA) appears as an important member of the series of small *N*-containing molecules.[7] Acting as a strong reductant, it can also be reduced depending on the conditions, and disproportionates readily through metal-catalyzed processes. HA is endogenously synthesized in mammals through the decomposition of nitrosothiols, and diverse metabolic roles have been investigated.[8] HA is frequently used as a NO-donor in experimental pharmacology.[8–10]

Given the involvement of transition metal centres, the coordination chemistry of HA has not been thoroughly investigated, particularly disproportionation reactions.[7] Recent work involving the catalytic role of pentacyano(aqua)ferrates[11] comprised the coordination of HA, redox cycling between Fe(II)–Fe(III) complexes, and the reactivity of radicals (*viz.*, the one-electron reduced NH_2 and oxidized NHOH species), thus determining the production of NH_3, N_2O, N_2 and bound NO^+. Some mechanistic ambiguities arose on the identity and role of the very reactive free radicals, and the formation of stable bound species before they were highlighted as acting as catalytic inhibitors (*viz.*, the coordination of diazene, N_2H_2, to the pentacyanoferrate fragment). In this present work, we address the influence of methyl-substitution in HA-coordination chemistry, given that *N*-methylhydroxylamine (MeHA) and *N,N*-dimethylhydroxylamine (Me_2HA) are also of chemical and biochemical interest.[8] There is a current interest in the influence of Me-substitution upon the reactivity of HA,[12] and it is known that the alkyl-derivatives significantly reduce the relaxant activity.[13] Besides, *N*-alkyl substitution has been shown to markedly prolong the lifetime of the corresponding nitroxide radicals,[14] which therefore could be more readily identified during the multi-electron processes leading to the reduced or oxidized x products. Among the latter, we look for the characterization of *C*-nitrosoalkanes,[15] which participate in the oxidative degradation of drugs or exogenous compounds containing an amine or hydroxylamine function and bind tightly to Fe(II), causing severe inhibition of the hepatic detoxifying cytochrome-activity.[16] These metal-mediated catalytic reactions are at the heart of the basic chemistry associated with the transformations of other reduced *N*-molecules like L-arginine,[4] hydroxyurea,[17] *etc.*, comprising the delivery of HNO, NO or NO_2^- to the biological fluids.

Experimental

Materials and methods

De-ionized water was used in all the experiments. *N*-methylhydroxylamine ($CH_3N(H)OH{\cdot}HCl$ >98%) and *N,N*-dimethylhydroxylamine ($(CH_3)_2NOH{\cdot}HCl$ >98%) were from Fluka. The solids were dried and stored in a desiccator over silica-gel. All other chemicals were of reagent grade. $Na_3[Fe^{II}(CN)_5NH_3]{\cdot}3H_2O$ was synthesized and purified according to literature procedures.[18] It was dried overnight in a vacuum desiccator over sulfuric acid, and

[a]*Department of Chemistry, Facultad de Ciencias Exactas y Naturales, Universidad Nacional de Mar del Plata, Funes y Roca, Mar del Plata, B7602AYL, Argentina. E-mail: amorebie@mdp.edu.ar*
[b]*Department of Inorganic, Analytical and Physical Chemistry and INQUIMAE, CONICET, Facultad de Ciencias Exactas y Naturales, Universidad de Buenos Aires, Pabellón 2, Ciudad Universitaria, C1428EHA, Buenos Aires, Argentina*

† Electronic supplementary information (ESI) available: ^1H and ^{13}C NMR spectra of the exhausted solutions of $[Fe(CN)_5H_2O]^{3-}$ with MeHA (Fig. S1–S2). ATR spectra of the reactive solution of $[Fe(CN)_5H_2O]^{3-}$ with [MeHA] (Fig. S3). FTIR transmittance spectra of the red solid in the reaction with MeHA (Fig. S4). Rate constants for the reaction of $[Fe(CN)_5H_2O]^{3-}$ with MeHA at different concentrations of reactants and pH (Table S1). EPR spectrum of the red solid obtained in the reaction of $[Fe(CN)_5H_2O]^{3-}$ with MeHA (Fig. S5). ^1H and ^{13}C NMR spectra of the exhausted solutions of $[Fe(CN)_5H_2O]^{3-}$ with Me_2HA (Fig. S6–S7). Rate constants for the reaction of $[Fe(CN)_5H_2O]^{3-}$ with Me_2HA at different concentrations of reactants and pH (Table S2). EPR spectrum of the solid obtained in the reaction of $[Fe(CN)_5H_2O]^{3-}$ with Me_2HA (Fig. S8). See DOI: 10.1039/b812173g

stored at 0 °C. Buffer solutions (20 mM KH_2PO_4–NaOH) covered the pH range 5.9–7.1 ± 0.2. The ionic strength (I) was adjusted to 1 M with NaCl. The $[Fe^{II}(CN)_5H_2O]^{3-}$ ion was generated *in situ* from $Na_3[Fe(CN)_5NH_3]\cdot 3H_2O$, by using weighed amounts of the solid in the argon-bubbled buffer solutions.[19] The solutions of MeHA and Me_2HA were generated similarly by using the above-stated commercial reagents. Formaldoxime and methylnitrone were prepared by mixing aqueous solutions of formaldehyde and hydroxylamine (or methylhydroxylamine) hydrochloride, to which sufficient sodium carbonate had been added to liberate the hydroxylamine.[20] The pH was adjusted to the desired value through an appropriate addition of solid KH_2PO_4–NaOH. The solutions were always maintained under argon bubbling and were used within 1 h of preparation to minimize possible decomposition of the reactants. The pH was determined at room temperature, *ca.* 20 °C, by using a digital pH/mV meter Hanna, model pH-211, with automatic temperature compensation, calibrated against Merck's standard buffers. A glass-body combination electrode (Hanna model HI 1131B) was employed.

For the characterization of intermediates and products, the concentration of $[Fe(CN)_5H_2O]^{3-}$ was typically 5–50 mM, and that of the substituted hydroxylamines was nearly equal. Electronic absorption spectra in the range 200–1000 nm were acquired on a diode array spectrophotometer, Ocean Optics, model HR 2000 CG UV-NIR, with quartz cells. The EPR spectra were obtained by mixing equal volumes of argon-purged reactant solutions on a 0.5 cm^3 flat, two-stream, fast-mixing flow cell of a stopped-flow device, mounted in the cavity, at room temperature. The X-band spectrometer (Bruker, model ER 200D) was calibrated by reference to TEMPO, 2,2,6,6-tetramethylpiperidine 1-oxyl, solutions (a = 1.72 mT, g = 2.0055, typically 1–5 μM)[21] or solid DPPH, 2,2-diphenyl-1-picrylhydrazyl (g = 2.0036).[22] The exhausted reaction mixtures in D_2O (Aldrich >95%), were analysed by ^1H and ^{13}C NMR spectroscopy with a Bruker 500 MHz instrument. The signals of CH_3OH or $NaCH_3COO$ were used as an internal reference. Chemical shifts are quoted in the δ scale, with downfield shifts positive. These solutions were also analysed by mass spectrometry (Extrel, model Emba II) in the positive ion electron impact mass spectral mode.[13] Reactive solutions were analysed by FTIR-HATR spectroscopy (Perkin-Elmer, model Spectrum BX), in a standard pre-mounted horizontal accessory with a flat sampling plate of ZnSe, spanning the 850–1550 and 1750–3100 cm^{-1} regions of the spectrum. The reactive solutions were treated with $ZnCl_2$ and a precipitate was obtained, containing a mixture of iron complexes. These solids were collected, washed with water, ethanol and diethyl ether, and dried in a vacuum desiccator. The IR spectra were measured with KBr disks.

The concentration of $[Fe(CN)_5H_2O]^{3-}$ employed in the substitution kinetic studies was typically 0.05–0.2 mM, and the concentration of the substituted hydroxylamine was always sufficiently large to ensure pseudo-first-order conditions. Equal volumes of the solutions were mixed in the cell of a stopped-flow accessory (Hi-Tech Scientific, model SFA-20), and were maintained at 25 ± 0.2 °C. Carefully controlled anaerobic conditions were employed in these experiments, since preliminary studies indicated rapid shifts of the bands of $[Fe^{II}(CN)_5H_2O]^{3-}$ (λ_{max} = 445 nm, ε = 660 M^{-1} cm^{-1}), suggesting conversion to $[Fe^{III}(CN)_5H_2O]^{2-}$ (λ_{max} = 395 nm, ε = 750 M^{-1} cm^{-1}).[19] Kinetic data were treated by standard data processing software. The quoted first order rate constants are the average of at least three runs. The possible influence of spurious ion catalysis was considered. The reactions were carried out in the absence and in the presence of 0.2 mM EDTA,[19] without any observable difference.

Results

All of the described chemical and spectral transformations of the alkylhydroxylamines require the presence of $[Fe(CN)_5H_2O]^{3-}$. No reactivity has been detected in its absence, or with the alternative addition of related $[Fe^{II}(CN)_5L]^{3-}$ complexes (L = CN^-, *S*-bound dimethylsulfoxide), in which the Fe^{II}–L bond remains particularly inert toward substitution.[23]

The reaction of $[Fe(CN)_5H_2O]^{3-}$ with *N*-methylhydroxylamine

By mixing anaerobic $[Fe(CN)_5H_2O]^{3-}$ with MeHA, two distinct processes can be observed depending on the medium conditions. With slightly substoichiometric MeHA, the initial yellow solution, characteristic of $[Fe(CN)_5H_2O]^{3-}$, turns reddish as the reaction progresses. A similar behaviour is observed by starting with a partially oxidized complex and an excess of MeHA, in buffer or unbuffered media (pH ~ 4). Moreover, the development of the red colour is favoured by oxygen bubbling throughout the reaction. The other process, with an excess of MeHA, shows that the buffered solutions of $[Fe(CN)_5H_2O]^{3-}$ (pH 6–8) turn to pale yellow as the reaction proceeds. We describe the two processes as evolving under oxidative or reductive conditions respectively. This characterization is performed in terms of the spectral evolution displayed in Fig. 3 and 4 (see later); *i.e.*, under the predominance of $[Fe^{III}(CN)_5H_2O]^{2-}$ or $[Fe^{II}(CN)_5H_2O]^{3-}$.

In both cases, either with the red or pale-yellow solutions generated in the EPR cell, a seven line weak spectrum is obtained, with relative line intensities of nearly 1:5:11:14:11:5:1 and g = 2.0054 (Fig. 1). This spectrum is interpreted as resulting from four equivalent hydrogens and one nitrogen atom, with all the hyperfine splittings equal to 1.38 mT. We assign it to the *N*-methylnitroxide

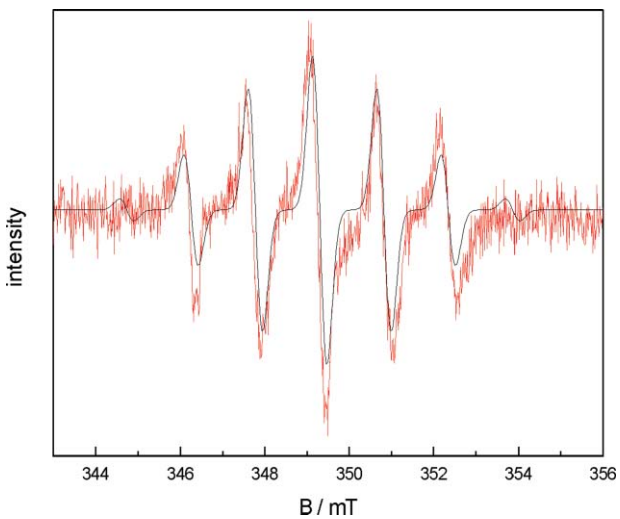

Fig. 1 EPR spectrum of the first radical observed in aqueous solution: 2.5 mM $[Fe(CN)_5H_2O]^{3-}$, 50 mM MeHA, at room temperature and pH 6.1 (I = 1 M, NaCl). Red line experimental, black line simulated spectra using the parameters reported in the text.

radical, $HN(CH_3)O$, in agreement with the experimental line intensities and reactivity reported in the literature.[24] The spectrum is not persistent, and is promptly replaced by another more complex signal, which vanishes in a few minutes (Fig. 2). We assign the second spectrum as arising from a mixture of radicals: $HN(CH_3)O$ and *N*-methyl-*N*-β-aminomethylnitroxide, $H_2N–CH_2–N(CH_3)O$, with $a_N(NO) = 1.6$, $a_H(CH_3) = 1.37$, $a_H(CH_2) = 0.93$, $a_N(NH_2) = 0.16$, $a_H(NH_2) = 0.045$ mT.[25]

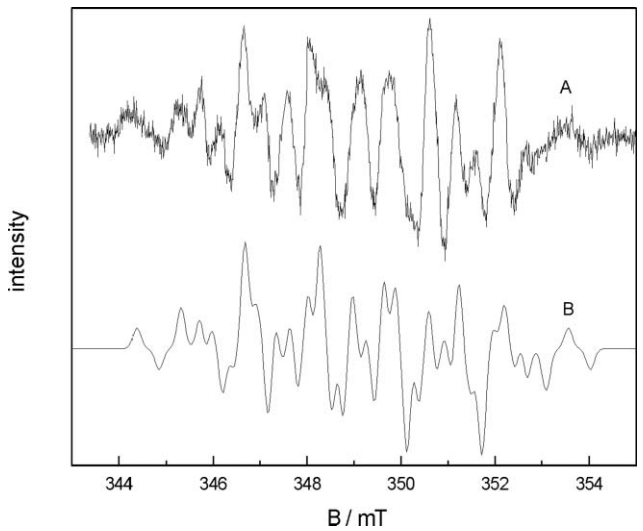

Fig. 2 EPR spectrum of the second radical observed in aqueous solution, same conditions as in Fig. 1. Experimental (A) and simulated (B) spectra of $H_2N–CH_2–N(CH_3)O$ radical using the parameters reported in the text.

At the end of the reactions, the exhausted solutions were analysed by mass spectrometry. The profiles appear complex, although the analysis of the more intense peaks indicates the production of azomethane ($CH_3N=NCH_3$) and azoxymethane ($CH_3N=N(CH_3)\rightarrow O$), both showing characteristic mass spectra, with molecular ions at $m/z = 58$ and 74 amu, respectively. Other fragments corresponding to these compounds were observed at $m/z = 43–28–15$ and 59–57–45–30 amu, respectively.

Subsequent confirmation was obtained by means of ^1H and ^{13}C NMR spectroscopy (see Table 1 and Fig. S1–S2†). Also, methylamine (CH_3NH_2) and formaldoxime ($CH_2=NOH$) have been identified as additional reaction products.

Fig. 3 shows the UV-visible spectra obtained under oxidative conditions in excess of MeHA, by starting the reaction with partially oxidized solutions of the aqua-complexes. These solutions were obtained in a few minutes by bubbling O_2 in the solutions of $[Fe(CN)_5H_2O]^{3-}$, followed by argon degassing. The initial spectrum shows two bands; one centred at 395 nm (ε = 750 M^{-1} cm^{-1}), and another centred at *ca.* 1400 nm. We can confidently assign these spectral features to the mixed-valence, cyano-

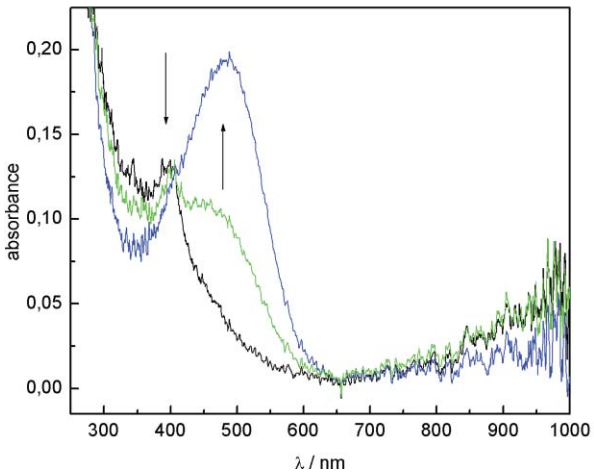

Fig. 3 Successive spectra during the reaction of 0.16 mM $Fe^{II,III}$ aqua–complexes with 3.4 mM MeHA at 25 °C and pH 6.1 (I = 1 M, NaCl). Initial (black line), 2 (green line) and 10 s (blue line) of reaction.

bridged complex $[(NC)_5Fe^{III}NCFe^{II}(CN)_4(H_2O)]^{5-}$.[26] Subsequent spectra show that the absorption at 1400 nm disappears with the advancement of the reaction, together with the decrease of the 395 nm band and the development of a new one centred at 487 nm ($\varepsilon > 3600$ M^{-1} cm^{-1}), with an isosbestic point at 410 nm. This band persists with some intensity during much of the reaction course.

ATR measurements were performed in order to isolate possible intermediates under substoichiometric MeHA conditions. The strong CN-stretching absorption (ν_{CN}) at *ca.* 2035 cm^{-1}, characteristic of initial $[Fe(CN)_5H_2O]^{3-}$,[27] shifts to 2079 cm^{-1} as the reaction progresses. In addition, a band system forms at 1500–1400 cm^{-1}, and another band appears at 1349 cm^{-1}. The transmittance FTIR of the dark red Zn-precipitate shows the previously described bands shifted to higher energies by *ca.* 10–15 cm^{-1}, as already observed elsewhere for Prussian-Blue type solids obtained by mixing the cyano-complexes with transition metals.[28] Thus, ν_{CN} is observed at 2090 cm^{-1}, with two low intensity bands that disappear in the hours time scale, at 1460 and 1359 cm^{-1} (Fig. S3–S4†). The latter bands can be tentatively attributed to CH-bending and to NO-stretching, ν_{NO}, respectively.[29,30]

The initial EPR spectrum of the red solid shows a broad triplet centred at 344 mT, with intensities of nearly 7:5:3 and $g \sim 2.038$. These signals decay after a few hours to a broad singlet centred at 350 mT with $g \sim 2.004$ (see Fig. S5†). Together with the IR result, which suggests that the red species is a nitrosomethane complex, $[Fe^{II}(CN)_5N(O)CH_3]^{3-}$ (see below),[25a,30] the EPR result points to the additional presence of its radical precursor, containing a bound methylnitroxide radical. Another possibility deals with the presence of a tautomeric form of bound CH_3NO, namely the EPR active $[Fe^{III}(CN)_5N(O)CH_3]^{3-}$.[31]

Table 1 ^1H and ^{13}C data relating to the reaction of $[Fe(CN)_5H_2O]^{3-}$ with MeHA

$\delta(^1H)_{calc}$ (ppm)	$\delta(^1H)_{exp}$ (ppm)	$\delta(^{13}C)_{calc}$ (ppm)	$\delta(^{13}C)_{exp}$ (ppm)	Assignment
2.47 (s)	2.56 (s)	27.80	24.6	CH_3NH_2
2.60 (s)	2.91 (s)	37.75	39.2	$CH_3N(H)OH$
3.44 (s)	3.72 (s)	46.89	51.35	*cis*-$CH_3N=NCH_3$ or $CH_3N=N(CH_3)\rightarrow O$
6.5 (dd)	6.83 (dd)	132.81	133.68	$CH_2=NOH$

Fig. 4 shows the successive UV-visible spectra obtained after mixing buffered reactant solutions at pH 6.1, under reductive conditions, in excess of MeHA. The decay of $[Fe(CN)_5H_2O]^{3-}$ is accompanied by the development of a new band centred at 338 nm ($\varepsilon > 2200$ M^{-1} cm^{-1}), with an isosbestic point at nearly 410 nm. The buildup of this band rapidly attains a high intensity, and is followed by a slow decay, suggesting a partial regeneration of $[Fe(CN)_5H_2O]^{3-}$ at 440 nm.

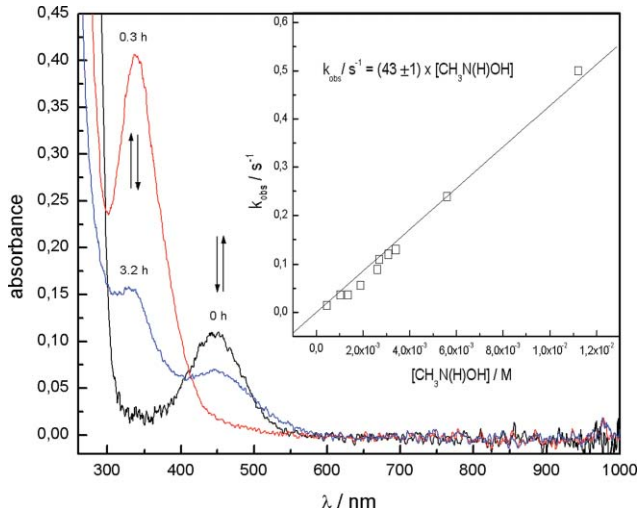

Fig. 4 Successive spectra during the reaction of 0.18 mM $[Fe(CN)_5H_2O]^{3-}$ with 3.6 mM MeHA, at 25 °C and pH 6.1 ($I = 1$ M, NaCl). 0 (black line), 0.3 (red line) and 3.2 h (blue line) of reaction.

Searching for intermediates, the reaction was carried out on the ATR flat plate. The spectrum of the initial solution shows ν_{CN} at 2035 cm^{-1} as before. The intensity of this signal decreases with time, and a CH bending region at 1500–1400 cm^{-1} appears. As the reaction was performed at a very high concentration of the complex and substoichiometric MeHA, weak bands of the red complex are also observed. The transmittance FTIR spectrum of the yellow Zn-solid also shows the general shift of the bands toward higher energies. No radical signals were observed in the EPR spectrum of the solid.

Kinetic measurements under pseudo-first-order conditions showed a single exponential decay at 445 nm, yielding k_{obs}. At constant pH, the plots of k_{obs} against the concentrations of free MeHA were linear, without a meaningful intercept (inset Fig. 4 and Table S1†). Thus, the rate law was: R (M s^{-1}) $= 43 \pm 4 \times$ [MeHA] $\times$ $[Fe(CN)_5H_2O^{3-}]$. The concentrations of free MeHA were estimated by using: $[MeHA] = [MeHA]_0/(1 + 10^{(pK_a - pH)})$; where $[MeHA]_0$ is the initial analytical concentration and pK_a has the usual meaning.

In order to characterize the iron compound absorbing at *ca.* 338 nm, we observed that buffered solutions of CH_2=NOH react with $[Fe(CN)_5H_2O]^{3-}$ generating a new species with absorption maximum at *ca.* 332 nm ($\varepsilon \geq 1600$ M^{-1} cm^{-1}). The plots of k_{obs} obtained from the decay at 445 nm were proportional to the concentration of CH_2=NOH, with an intercept, yielding: R (M s^{-1}) $= 124 \pm 5 \times$ [CH_2=NOH] $\times$ $[Fe(CN)_5H_2O^{3-}]$. The iron compound absorbing at 338 nm could be tentatively ascribed to the bound CH_2=NOH and the $HN(CH_3)O$ radical.

Table 2 ^1H and ^{13}C data relating to the reaction of $[Fe(CN)_5H_2O]^{3-}$ with Me_2HA

$\delta(^1H)_{calc}$ (ppm)	$\delta(^1H)_{exp}$ (ppm)	$\delta(^{13}C)_{calc}$ (ppm)	$\delta(^{13}C)_{exp}$ (ppm)	Assignment
2.32 (s)	2.56 (s)	38.2	34.44	$(CH_3)_2NH$
2.61 (s)	2.98 (s)	49.94	47.67	$(CH_3)_2NOH$
2.85 (d)	2.67 (d)	50.4	50	$((CH_3)_2NO)_2$
4.1 (s)–5.9 (dd)	4.75 (d)	53.67–137.56	24.6–81.54	CH_2=N(CH_3)→O

The reaction of $[Fe(CN)_5H_2O]^{3-}$ with *N*,*N*-dimethylhydroxylamine

By mixing solutions of $[Fe(CN)_5H_2O]^{3-}$ with an excess of Me_2HA, a reaction takes place. It evolves in the same way as with MeHA under substoichiometric conditions, or if oxidized $Fe^{II,III}$ mixtures are used as starting materials. The observed reaction products, identified by ^1H and ^{13}C NMR chemical shifts, were dimethylamine, $(CH_3)_2NH$, and methylnitrone, CH_2=N(CH_3)→O (see Table 2, Fig. S6–S7†).

The global reaction can be described by eqn (1)

$$2(CH_3)_2NOH \rightarrow CH_2{=}N(CH_3){\rightarrow}O + (CH_3)_2NH + H_2O \quad (1)$$

Fig. 5 displays the EPR results, with a fast development of a moderately intense spectrum 1:6:15:20:20:20:15:6:1 (and minor hyperfine splitting with 21 signals in total), with $g = 2.0058$. We interpret the spectrum as resulting from six equivalent hydrogens with the hyperfine splitting $a_H(CH_3) = 1.50$ mT and a N-atom with $a_N(NO) = 1.65$ mT. The assignment to the dimethylnitroxide radical, $(CH_3)_2NO$, is consistent with reactivity, experimental line intensities, and previous literature reports.[24a–c,32] This radical persists with a high intensity during nearly all the reaction time.

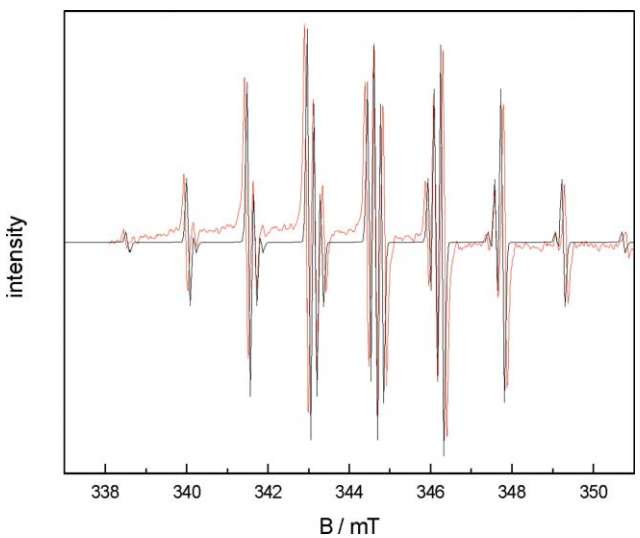

Fig. 5 EPR spectrum for the reaction of 2.5 mM $[Fe(CN)_5H_2O]^{3-}$ with 25 mM Me_2HA, at room temperature, pH 6.1 ($I = 1$ M, NaCl). Experimental (red line) and simulated (black line) spectra using the parameters reported in the text.

The UV-visible spectral evolution of the reaction was similar to the one displayed in Fig. 4. The decay at 445 nm is accompanied by the development of a band centred at 338 nm. The buildup of this band, rapidly attaining high intensity, is again followed by a slow decay with partial regeneration of $[Fe(CN)_5H_2O]^{3-}$. In the

kinetic experiments, the absorption at 445 nm shows a first-order decay, yielding k_{obs} (Table S2†). At constant pH, the plot of k_{obs} against the concentration of free Me_2HA was linear, without a meaningful intercept, allowing for the calculation of the following kinetic law: $R\,(M\,s^{-1}) = 4.4 \pm 0.5 \times [Me_2HA] \times [Fe(CN)_5H_2O^{3-}]$. The concentrations of free Me_2HA were estimated using: $[Me_2HA] = [Me_2HA]_0/(1 + 10^{(pK_a - pH)})$; where $[Me_2HA]_0$ is the initial analytical concentration.

The iron compound absorbing at 338 nm is tentatively ascribed to the bound $(CH_3)_2NO$ radical. We observed that aqueous solutions of $CH_2{=}N(CH_3){\rightarrow}O$ *do not react* with $[Fe(CN)_5H_2O]^{3-}$ (in contrast with formaldoxime, see above). When $[Fe(CN)_5H_2O]^{3-}$ is treated with substoichiometric Me_2HA, the transmittance ATR spectrum shows ν_{CN} at 2035 cm^{-1}, with a decrease in intensity as the reaction progresses, and a new band system emerging at 1400–1500 cm^{-1}, tentatively assignable to CH_3-bending. The EPR spectrum of the Zn-containing solid (Fig. S8†) shows a broad three line structure centered at *ca.* 343 mT with intensities of nearly 7:5:3 and $g \sim 2.046$. These signals were relatively persistent in anhydrous conditions, and may be confidently assigned to the bound $(CH_3)_2NO$ radical.

When the reaction is performed at slightly substoichiometric Me_2HA, the production of Fe^{III} species is evidenced through the UV-visible spectra, as was the case with MeHA.

Catalysis

In all reaction conditions, the analysis of the exhausted solutions indicates a catalytic process with total consumption of the alkylhydroxylamines. The active and formal concentrations of $[Fe(CN)_5H_2O]^{3-}$ are different in each case because the species absorbing at 338 and/or 487 nm act as bottle-necks of the catalytic cycle. The time evolution of all the products were not measured in the whole set of experiments. Under reaction conditions the products are stable species, although they hydrolyse to formaldehyde, $CH_2{=}O$, and other species in strong acid medium. Therefore, the catalysis was followed by quantifying $CH_2{=}O$ with chromotropic acid,[33] as shown in Fig. 6 for several initial conditions. This reaction is specific for $CH_2{=}O$ and shows no known interferences. The plots are fairly linear with up to more than 50% consumption of MeHA. Referring to the distribution of products at constant complex-concentration, the production of $CH_2{=}O$ is almost insensitive to the pH (curves A and B) and to the analytical concentration of MeHA (curves C and D). However, at constant concentration of MeHA, the yield of $CH_2{=}O$ increases with the complex-concentration (curves B and C). As the reactions are relatively slow, the influence of atmospheric oxygen on the rate and yield of products has been assessed. Oxygen increases the yield of the oxidation products, $CH_2{=}NOH$ and $CH_3N{=}N(CH_3){\rightarrow}O$, at the expense of CH_3NH_2 and $CH_3N{=}NCH_3$ (curve E). As shown in the inset of Fig. 6, the plot of the rate of $CH_2{=}O$ production against the analytical concentration of $[Fe(CN)_5H_2O]^{3-}$ is reasonably linear, yielding: $R_{CH_2=NOH}$ $(M\,s^{-1}) = 1.7 \pm 0.2 \times 10^{-4} \times [Fe(CN)_5H_2O^{3-}]_0$. Although the real reaction rates ought to be divided by the fractions of produced $CH_2{=}NOH$ (which were not measured in all the experiments), we consider the $CH_2{=}O$ rates to be a reasonable trace of the overall kinetics. The kinetic law for the catalysis is probably indicative of a rate-determining step of first order in iron and zero order, or saturation, in MeHA.

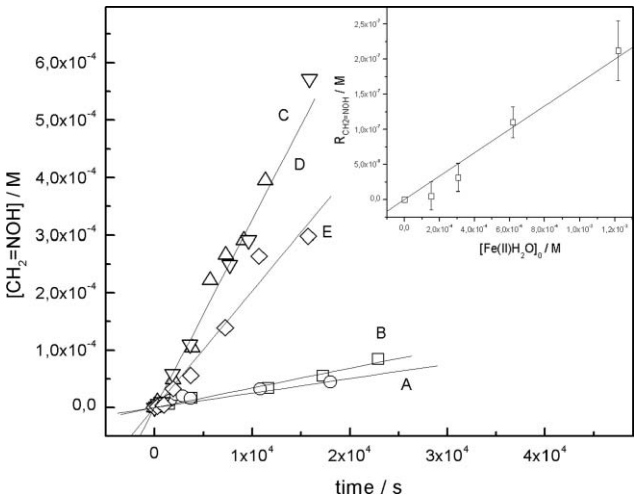

Fig. 6 Evolution of the concentration of $CH_2{=}O$ against time at 25 °C ($I = 1$ M, NaCl): (A) 0.15 mM $[Fe(CN)_5H_2O]^{3-}$, 2.3 mM MeHA, pH 7.2; (B) 0.15 mM $[Fe(CN)_5H_2O]^{3-}$, 2.5 mM MeHA, pH 6.2; (C) 0.31 mM $[Fe(CN)_5H_2O]^{3-}$, 5.0 mM MeHA, pH 6.2; (D) 0.31 mM $[Fe(CN)_5H_2O]^{3-}$, 2.5 mM MeHA, pH 6.2; (E) 0.15 mM $[Fe(CN)_5H_2O]^{3-}$, 2.3 mM MeHA, pH 7.2; oxygen saturated.

The extent of the catalysis for Me_2HA was monitored by measuring the time evolution of the concentration of $CH_2{=}N(CH_3){\rightarrow}O$. This compound is stable in the reaction conditions. However, it hydrolyses fast to $CH_2{=}O$ and probably to MeHA in strong acid medium. The $CH_2{=}O$ production was quantified as before. We verified negative $CH_2{=}O$ tests for $(CH_3)_2NH$, MeHA, and when the reaction was conducted in the absence of $[Fe(CN)_5H_2O]^{3-}$. The observed time evolution was similar to the one shown in Fig. 6 for MeHA.

The concentration of $[Fe(CN)_5H_2O]^{3-}$ did not remain constant during the full course of the reaction. However the plot of the rates of $CH_2{=}N(CH_3){\rightarrow}O$ production (quantified as $CH_2{=}O$) against the analytical concentration of $[Fe(CN)_5H_2O]^{3-}$ is reasonably linear, yielding: $R_{CH_2=N(CH_3)\rightarrow O}$ $(M\,s^{-1}) = 2.1 \pm 0.2 \times 10^{-4} \times [Fe(CN)_5H_2O^{3-}]_0$. As the fraction of $CH_2{=}N(CH_3){\rightarrow}O$ was 0.5 of the total consumed Me_2HA, the overall reaction rate requires the division of $R_{CH_2=N(CH_3)\rightarrow O}$ by 0.5. Here again, as the reaction is relatively slow, the influences of pH and oxygen on the rate and yield of products were assessed. The pH has no effect, and oxygen increases the yield of $(CH_2{=}N(CH_3){\rightarrow}O)$ at the expense of $(CH_3)_2NH$.

Discussion

According to the pK_a's for MeHA and Me_2HA (5.9 and 5.5, respectively),[34] both protonated and deprotonated species are in equilibrium under our reaction conditions. Upon dissolution of solid $Na_3[Fe(CN)_5NH_3]{\cdot}3H_2O$, the fast production of $[Fe(CN)_5H_2O]^{3-}$ must occur in a few minutes ($t_{1/2}$ = *ca.* 40 s),[19] eqn (2):

$$[Fe^{II}(CN)_5NH_3]^{3-} + H_2O \leftrightarrow [Fe^{II}(CN)_5H_2O]^{3-} + NH_3 \qquad (2)$$

At pH 6.1–7.1, NH_3 and the produced amines $CH_3N(R)H$ (R = H, CH_3) remain protonated, as the pK_a's are in the range

9–11,[35] thus allowing the aquation of the amino-complexes. At high complex-concentrations the reactant system may contain associated species, starting with reaction (3):

$$2[Fe^{II}](CN)_5H_2O]^{3-} \leftrightarrow [(NC)_5Fe^{II}NCFe^{II}(CN)_4(H_2O)]^{6-} + H_2O \quad (3)$$

The establishment of equilibrium (3) comprises of relatively slow transformations (hours time scale). The persistence of the monomer is always guaranteed in our reaction conditions. Besides, the oxidizing conditions, eventually prevailing in the reaction medium, may allow for the presence of $[Fe^{III}(CN)_5H_2O]^{2-}$,[19] or the corresponding oxidized dimers (Fe^{II},Fe^{III} or Fe^{III},Fe^{III}).[26] These conditions become more evident in the presence of O_2, which oxidizes the metal centre.

We propose the main reaction course in Scheme 1, with emphasis on the intermediates and products generated under reductive conditions, *i.e.* excess MeHA or Me_2HA, and anaerobic media. We expand on this reaction course below, as well as considering the significant variations found when the underlying reaction conditions are changed. We emphasize the role of radical (free or bound) intermediates in the mechanism, and provide evidence for supporting a catalytic process for the disproportionation of MeHA and Me_2HA, given that the active catalyst $[Fe(CN)_5H_2O]^{3-}$ is regenerated along the process.

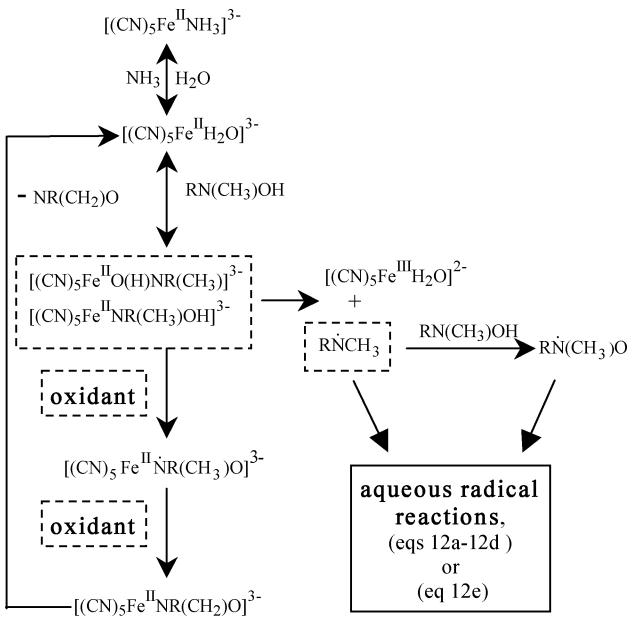

Scheme 1 Dashed boxes enclose intermediates that were not characterized.

The initial reactivity must involve a coordination step, favoured by the lability of the aqua-ligand in $[Fe(CN)_5H_2O]^{3-}$.[23] Kinetic evidence on the decay of the latter species, measured by the observed second-order rate constants, is consistent with values obtained for reactions of similar L ligands binding to $[Fe(CN)_5H_2O]^{3-}$, in a process that is rate-controlled by the loss of water from the iron-complex.[36] The observed unreactivity with other $[Fe^{II}(CN)_5L]^{n-}$ complexes can be explained on the basis of the substitutionally inert Fe^{II}–L bonds, even though the redox potentials of the corresponding $Fe^{III,II}$ redox couples are of similar magnitude, including the one for $[Fe^{III,II}(CN)_5H_2O]^{2,3-}$ (*ca.* 0.4 V *vs.* SHE).[23]

We consider two alternative coordination modes for $RN(CH_3)OH$ (R = H or CH_3 for MeHA and Me_2HA):[7,13]

$$[Fe^{II}(CN)_5H_2O]^{3-} + RN(CH_3)OH \leftrightarrow [Fe^{II}(CN)_5O(H)NR(CH_3)]^{3-} + H_2O \quad (4a)$$

$$[Fe^{II}(CN)_5H_2O]^{3-} + RN(CH_3)OH \leftrightarrow [Fe^{II}(CN)_5NR(CH_3)OH]^{3-} + H_2O \quad (4b)$$

Given the UV-visible evidence on the fast generation of Fe^{III}, *even under anaerobic conditions*, we propose a fast follow-up to reaction (4a), namely an intramolecular homolytic dissociation reaction, eqn (5):

$$[Fe^{II}(CN)_5O(H)NR(CH_3)]^{3-} + H^+ \rightarrow [Fe^{III}(CN)_5H_2O]^{2-} + R\dot{N}CH_3 \quad (5)$$

Evidence for the aminyl radical in reaction (5) is provided by the production of the β-aminonitroxide radical.[25] It has been demonstrated that *N*-alkylaminyl radicals, R_2CHNH, rearrange rapidly to α-aminoalkyl radicals, R_2CNH_2, which then react with nitrosoalkanes, R′NO, giving β-aminonitroxide radicals, $H_2NCR_2NR'O$.[25b] Therefore, the secondary EPR spectrum in Fig. 2 for the reaction of MeHA should correspond to the aminonitroxide formed from CH_2NH_2 and CH_3NO.

Additional evidence for the $R\dot{N}CH_3$ intermediate is supplied by the production of azomethane (see below).

The product in reaction (4b) may be oxidized by Fe^{III}, giving the one-electron oxidized nitroxide bound radical, eqn (6). This radical may be further oxidized to relatively stable, two-electron oxidized products, namely formaldoxime (R = H) or methylnitrone ($R = CH_3$) eqn (7):

$$[Fe^{III}(CN)_5H_2O]^{2-} + [Fe^{II}(CN)_5NR(CH_3)OH]^{3-} \rightarrow [Fe^{II}(CN_5)H_2O]^{3-} + [Fe^{II}(CN)_5\dot{N}R(CH_3)O]^{3-} + H^+ \quad (6)$$

$$[Fe^{III}(CN)_5H_2O]^{2-} + [Fe^{II}(CN)_5\dot{N}R(CH_3)O]^{3-} \rightarrow [Fe^{II}(CN_5)H_2O]^{3-} + [Fe^{II}(CN)_5NR(CH_2)O]^{3-} + H^+ \quad (7)$$

Reaction (7) explains the absorption properties of the final product in Fig. 4 (maximum at 338 nm). Independent kinetic experiments for the coordination of formaldoxime to $[Fe(CN)_5H_2O]^{3-}$ support this assignment, although we cannot discard some contribution of the radical nitroxide complex in eqn (6) to the absorption profile. Thus, Scheme 1 describes the generation of the *N*-bound species as arising from the presence of an oxidizing pool, which certainly may not only be comprised of Fe^{III} complexes, but also of $R\dot{N}CH_3$ radicals formed in reaction (5). Reactions (8)–(11) describe this behaviour, forming the corresponding amines, as demonstrated by NMR spectroscopy.

$$[Fe^{II}(CN)_5NR(CH_3)OH]^{3-} + R\dot{N}CH_3 \rightarrow [Fe^{II}(CN)_5\dot{N}R(CH_3)O]^{3-} + RN(CH_3)H \quad (8)$$

$$[Fe^{II}(CN)_5\dot{N}R(CH_3)O]^{3-} + R\dot{N}CH_3 \rightarrow [Fe^{II}(CN)_5NR(CH_2)O]^{3-} + RN(CH_3)H \quad (9)$$

$$RN(CH_3)OH + R\dot{N}CH_3 \rightarrow R\dot{N}(CH_3)_5O + RN(CH_3)H \quad (10)$$

$$[Fe^{II}(CN)_5H_2O]^{3-} + R\dot{N}CH_3 + H^+ \rightarrow [Fe^{III}(CN)_5H_2O]^{2-} + RN(CH_3)H \quad (11)$$

Reaction (10), arising in the oxidizing ability of the aminyl radicals,[37] constitutes the main source of nitroxide radicals. This is supported by the calculated isotropic *g* values (see Results), typical of species with low electron delocalization, and thus should be assigned to *non iron-bonded* radicals. On the other hand, the *g* values of the radicals detected in the red Zn-precipitates of the reactive solutions are consistent with a high electron delocalization, and support their assignment as bound-species, as in eqn (6) or (8).[38] The bound formaldoxime product in reactions (7) and (9) (R = H) is moderately stable ($k_{diss} \leq 2 \times 10^{-2}$ s^{-1}) and apparently regulates the concentration of active centres by means of the release of CH_2=NOH to the medium.

The chemistries of the free nitroxide-radicals $HN(CH_3)O$ and $(CH_3)_2NO$ are quite different. In the reaction with MeHA, the reactivity of $HN(CH_3)O$ is described by reactions (12a)–(12d), accounting for the diversified pattern of products:

$$H\dot{N}(CH_3)O + HN(CH_3)OH \rightarrow CH_2{=}NOH + H\dot{N}CH_3 + H_2O \quad (12a)$$

$$H\dot{N}(CH_3)O + H\dot{N}CH_3 \rightarrow CH_3N{=}NCH_3 + H_2O \quad (12b)$$

$$H\dot{N}(CH_3)O + H\dot{N}(CH_3)O \rightarrow CH_3N{=}N(CH_3){\rightarrow}O + H_2O \quad (12c)$$

$$H\dot{N}(CH_3)O + H\dot{N}(CH_3)OH \rightarrow HN(CH_3)OH + CH_2{=}NOH \quad (12d)$$

The $(CH_3)_2NO$ radicals decay slowly by disproportionation, eqn (12e):

$$(CH_3)_2\dot{N}O + (CH_3)_2\dot{N}O \rightarrow N(CH_3)_2OH + CH_2{=}N(CH_3){\rightarrow}O \quad (12e)$$

In partially oxidized solutions of the iron-complex, or when the reactions start with anaerobic substoichiometric MeHA, the mixed-valence Fe^{II}, Fe^{III} dimer is initially observed. The spectral evolution (Fig. 3) suggests dimer dissociation and the production of $[Fe^{II}(CN)_5N(O)CH_3]^{3-}$, which is also observed at high reactant concentrations, under oxidative conditions. Some precedent exists on the coordination of nitrosoalkanes to pentacyanoferrate(II).[25a,30] The identification of $[Fe^{II}(CN)_5N(O)CH_3]^{3-}$ can be seen in the UV-visible spectrum (Fig. 3, intense MLCT band, as also seen with related RN=O ligands, with R = $CH_2C(CH_3)_2OH$,[30b] hydrogen,[39] benzyl,[40] thiolates[41]), and more conclusively through the assignment of ν_{NO}, which is systematically found at *ca.* 1300–1400 cm^{-1} for the above mentioned ligands containing the N=O group bound to Fe(II).[30b,39,41] Tautomerization processes are possible between the two-electron oxidized species of MeHA: formaldoxime (CH_2=NOH), nitrosomethane (CH_3NO), and the nitrone (CH_2=N(H)→O).[15] It has been calculated that formaldoxime is ~15.8 kcal mol^{-1} more stable than nitrosomethane, including a correction for water solvation. The formation of formaldoxime can be favoured by acid/base catalysis, thus explaining the product formation in Fig. 4. Considering the relative significance of the metal-bound and aqueous radical reactions for MeHA disproportionation, the H mass balance of the NMR spectrum (Fig. S1†) accounts for 20% of azomethane and azoxymethane production. In terms of the proposed mechanism, we infer that nearly 40% of MeHA might be processed by the aqueous radical reactions.

Conclusions

With $[Fe(CN)_5NH_3]^{3-}$ as the catalyst precursor, great amounts of alkylhydroxylamines can be processed, and with $[Fe(CN)_5H_2O]^{3-}$ as the cycling catalyst, disproportionation to the corresponding alkylamines and oxidation products occurs. Alternative *O*- or *N*-coordination to $[Fe(CN)_5H_2O]^{3-}$, further iron oxidation, and production of free $RNCH_3$ radicals (R = H or CH_3), set the basis for the catalysis. Indirect, though significant evidence for the involvement of free $RNCH_3$ radicals is provided by the detection of β-aminonitroxide radicals, which form under high concentration of reactants, or by starting with partially oxidized solutions of the iron-complex. The free $RNCH_3$ radicals decay quickly by abstraction of the α-hydrogen from the precursors, yielding the nitroxide radicals, $RN(CH_3)O$ (R = H or CH_3), which have been detected and characterized by EPR spectroscopy. The conditions for the stabilization of two-electron oxidation bound products have been elucidated. Thus, for the reaction of MeHA, bound CH_3NO has been well characterized. Although it is an unstable isomer, it is proposed to be formed under conditions favouring fast successive one-electron oxidations (free CH_3NO, not hindered around the N-atom, is very unstable). Changing the medium conditions favour the formation of the more stable CH_2=NOH, formaldoxime. The third nitrone isomer is absent for the reaction of MeHA, although the methylnitrone does form as the stable two-electron oxidized product for Me_2HA. Catalysis is somewhat inhibited by the endogenously formed, moderately strong ligands: CH_2=NOH and CH_3NO; although we cannot discard some contribution of the radical nitroxides.

By comparing with HA which formed N_2, HNO, N_2O and even NO^+ as oxidation products, the present work shows that the formation of stable products are limited to the +1 oxidation level, revealing significant mechanistic differences associated with the strong N–C bonds and the absence of deprotonation steps.

Acknowledgements

This work has been supported by the University of Mar del Plata, ANPCYT and CONICET. V.T.A. and J.A.O. are members of the scientific staff of CONICET. We thank Prof. Fabio Doctorovich and Lic. E. R. de Celis for the help received during the course of this work.

Notes and references

1 F. A. Cotton and G. Wilkinson, *Advanced Inorganic Chemistry*, Wiley, New York, 4th edn, 1980.
2 B. A. Averill, *Chem. Rev.*, 1996, **96**, 2951.
3 A. B. Hooper, in *Autotrophic Bacteria*, ed. H. G. Schlegel and B. Bowien, Science Tech. Publishers, Madison, WI, 1989.
4 P. A. Bush, N. E. González, J. M. Griscavage and L. J. Ignarro, *Biochem. Biophys. Res. Commun.*, 1992, **185**, 960.
5 *Cytochrome P450: Structure, Mechanism, and Biochemistry*, ed. P. R. Ortiz de Montellano, Plenum Press, New York, 3rd edn, 2004.
6 (*a*) M. P. Hendrich, M. Logan, K. K. Andersson, D. M. Arciero, J. D. Lipscomb and A. L. Hooper, *J. Am. Chem. Soc.*, 1994, **116**, 11961; (*b*) O. Einsle, A. Messerschmidt, R. Huber, P. M. H. Kroneck and F. Neese, *J. Am. Chem. Soc.*, 2002, **124**, 11737.
7 K. Wieghardt, *Adv. Inorg. Bioinorg. Mech.*, 1984, **3**, 213.
8 *Methods in Nitric Oxide Research*, ed. M. Feelisch and J. S. Stamler, Wiley, Chichester, 1996, ch. 1,2,7.
9 P. A. Craven, F. R. DeRubertis and D. W. Pratt, *J. Biol. Chem.*, 1979, **254**, 8213.

10 P. G. Wang, M. Xian, X. Tang, X. Wu, Z. Wen, T. Cai and A. J. Janczuk, *Chem. Rev.*, 2002, **102**, 1091.
11 G. B. Alluisetti, A. E. Almaraz, V. T. Amorebieta, F. Doctorovich and J. A. Olabe, *J. Am. Chem. Soc.*, 2004, **126**, 13432.
12 M. M. Gutiérrez, G. B. Alluisetti, J. A. Olabe and V. T. Amorebieta, *Dalton Trans.*, 2008, 5025.
13 G. Thomas and P. W. Ranwell, *Biochem. Biophys. Res. Commun.*, 1989, **164**, 889.
14 K. Stolze and H. Nohl, *Biochem. Pharmacol.*, 1989, **38**, 3055.
15 (*a*) J. Lee, L. Chen, A. H. West and G. B. Richter-Addo, *Chem. Rev.*, 2002, **102**, 1019; (*b*) G. B. Richter-Addo, *Acc. Chem. Res.*, 1999, **32**, 529.
16 D. Mansuy, P. Battioni, J. C. Chottard, C. Riche and A. Chiaroni, *J. Am. Chem. Soc.*, 1983, **105**, 455.
17 S. B. King, *Curr. Top. Med. Chem.*, 2005, **5**, 665.
18 D. J. Kenney, T. P. Flynn and J. B. Gallini, *J. Inorg. Nucl. Chem.*, 1961, **20**, 75.
19 H. E. Toma, *Inorg. Chim. Acta*, 1975, **15**, 205.
20 M. G. Krishna Pillai, *J. Phys. Chem.*, 1962, **66**, 179.
21 J. J. Testa, M. A. Grela and M. I. Litter, *Environ. Sci. Technol.*, 2004, **38**, 1589.
22 B. H. J. Bielski and J. M. Gebicki, *Atlas of Electron Spin Resonance Spectra*, Academic Press, New York, London, 1967.
23 J. A. Olabe, *Adv. Inorg. Chem.*, 2004, **55**, 61.
24 (*a*) J. Q. Adams, S. W. Nicksic and J. R. Thomas, *J. Chem. Phys.*, 1966, **45**, 654; (*b*) R. Poupko, A. Loewenstein and B. L. Silver, *J. Am. Chem. Soc.*, 1971, **93**, 580; (*c*) K. Stolze and L. Nohl, *Free Radical Res. Commun.*, 1990, **8**, 123; (*d*) D. F. Bowman, J. L. Brokenshire, T. Gillan and K. U. Ingold, *J. Am. Chem. Soc.*, 1971, **93**, 6551.
25 (*a*) W. A. Waters, *J. Chem. Soc., Perkin Trans. 2*, 1976, 732; (*b*) N. H. Anderson and R. O. Norman, *J. Chem. Soc. B*, 1971, 993.
26 (*a*) G. Emschwiller and C. K. Jorgensen, *Chem. Phys. Lett.*, 1970, **5**, 561; (*b*) M. F. Souto, F. D. Cukiernik, P. Forlano and J. A. Olabe, *J. Coord. Chem.*, 2001, **54**, 343; (*c*) G. Emschwiller, *Acad. Sci., Paris, C. R.*, 1967, **265**, 281.
27 P. J. Morando, V. I. E. Bruyère, M. A. Blesa and J. A. Olabe, *Transition Met. Chem.*, 1983, **8**, 999.
28 H. Inoue, T. Kawai, M. Nagao and S. Yanagisawa, *Bull. Chem. Soc. Jpn.*, 1982, **55**, 733.
29 G. Socrates, *Infrared, Characteristic Group Frequencies. Tables and Charts*, Wiley, New York, 2nd edn, 1998.
30 (*a*) R. P. Cheney, S. D. Pell and M. Z. Hoffman, *J. Inorg. Nucl. Chem.*, 1979, **41**, 489–493; (*b*) R. P. Cheney, M. G. Simic, M. Z. Hoffman, I. A. Taub and K. D. Asmus, *Inorg. Chem.*, 1977, **16**, 2187.
31 (*a*) J. N. Armor, R. Furman and M. Z. Hoffman, *J. Am. Chem. Soc.*, 1975, **97**, 1737; (*b*) W. Beck, K. Schmidtner and H. J. Keller, *Chem. Ber.*, 1967, **100**, 503.
32 (*a*) K. Adamic, D. F. Bowman, T. Gillan and K. U. Ingold, *J. Am. Chem. Soc.*, 1971, **93**, 902; (*b*) D. F. Bowman, T. Gillan and K. U. Ingold, *J. Am. Chem. Soc.*, 1971, **93**, 6555; (*c*) D. F. Bowman, T. Gillan and K. U. Ingold, *J. Am. Chem. Soc.*, 1970, **92**, 1093.
33 *NIOSH Manual of Analytical Methods*, Method No. 3500, 4th edn, 1994.
34 T. C. Bissot, R. W. Parry and D. H. Campbell, *J. Am. Chem. Soc.*, 1957, **79**, 796.
35 J. A. Dean, *Lange's Handbook of Chemistry*, Mc Graw-Hill, New York, 14th edn, 1992.
36 H. E. Toma and J. M. Malin, *Inorg. Chem.*, 1973, **12**, 2080.
37 (*a*) *Free Radicals*, ed. J. K. Kochi, Wiley, New York, 1973, vol. 2; (*b*) D. A. Armstrong, A. Rauk and D. Yu, *J. Am. Chem. Soc.*, 1993, **115**, 666.
38 F. Gerson and W. Huber, *Electron Spin Resonance Spectroscopy of Organic Radicals*, Wiley-VCH Verlag GmbH & Co. KGaA, Weinheim, 2003.
39 M. González Lebrero, D. A. Scherlis, G. L. Estiú, J. A. Olabe and D. A. Estrin, *Inorg. Chem.*, 2001, **40**, 4127.
40 H. Kunkely and A. Vogler, *J. Photochem. Photobiol., A*, 1998, **114**, 197.
41 J. D. Schwane and M. T. Ashby, *J. Am. Chem. Soc.*, 2002, **124**, 6822.

